

Multiplex Structures: Patterns of Complexity in Real-World Networks

Bo Yang¹, Jiming Liu²

¹*Jilin University, Changchun city, China. Email: ybo@jlu.edu.cn*

²*Hong Kong Baptist University, Hong Kong. Email: jiming@comp.hkbu.edu.hk*

Complex network theory aims to model and analyze complex systems that consist of multiple and interdependent components. Among all studies on complex networks, topological structure analysis is of the most fundamental importance, as it represents a natural route to understand the dynamics, as well as to synthesize or optimize the functions, of networks. A broad spectrum of network structural patterns have been respectively reported in the past decade, such as communities, multipartites, hubs, authorities, outliers, bow ties, and others. Here, we show that most individual real-world networks demonstrate multiplex structures. That is, a multitude of known or even unknown (hidden) patterns can simultaneously situate in the same network, and moreover they may be overlapped and nested with each other to collaboratively form a heterogeneous, nested or hierarchical organization, in which different connective phenomena can be observed at different granular levels. In addition, we show that the multiplex structures hidden in exploratory networks can be well defined as well as effectively recognized within an unified framework consisting of a set of proposed concepts, models, and algorithms. Our findings provide a strong evidence that most real-world complex systems are driven by a combination of heterogeneous mechanisms that may col-

laboratively shape their ubiquitous multiplex structures as we observe currently. This work also contributes a mathematical tool for analyzing different sources of networks from a new perspective of unveiling multiplex structures, which will be beneficial to multiple disciplines including sociology, economics and computer science.

1 Introduction

Complex network analysis provides a novel approach to examining how networked systems in nature are originated and evolving according to what basic principles, and moreover armed with such discovered principles, constructing efficient, robust as well as flexible man-made networked systems under different constraints. Among all studies about complex networks, structure analysis is the most fundamental, and the ability to discover and visualize the underlying structure of a real-world network in question will be greatly helpful for both topological and dynamic analysis applied to it ¹. So far, scientists have uncovered a multitude of structural patterns ubiquitously existing in social, biological, ecological or technological networks; they may be microscopic such as motifs ², mesoscopic such as modularities³ or macroscopic such as small world ⁴ and scale-free phenomena ⁵. These structural patterns observed at different granular levels may collectively unveil the secrets hidden in complex networked systems. All these works have greatly triggered the common interesting as well as boosted the progress of exploring complex networks in both scientific and engineering domains. However, the topological structure analysis of complex networks, even restricted to the mesoscopic level, remains one of the major challenges in network theory mainly because most of the real-world networks are usually resulted from a combination

of heterogeneous mechanisms which may collaboratively shape their non-trivial structures. More specifically one can raise the following issues.

Above all, beyond modularity the most extensively studied at the mesoscopic level ^{3,6}, a wide spectrum of structural patterns have been reported in the literature including bipartites or more generally multipartites ⁷⁻⁹, hubs, authorities and outliers ¹⁰⁻¹², bow ties ¹³⁻¹⁵ or others. Moreover, these miscellaneous patterns may simultaneously coexist in the same networks, or they may even overlap with each other such as the overlaps between communities ¹⁶. Fig. 1 shows an illustrative example, in which a social network encoding the co-appearances of 77 characters in the novel "Les Misérables" is visualized in terms of both network and matrix representations. One would observe two hubs and a number of outliers coexisting with four well-formed communities. The two hubs, corresponding to *Valjean* and *Javert*, are the main characters of the novel, and their links are across all other clusters by connecting about 48% of the overall characters. It indicates that the two roles interacting with different characters in different chapters are the two main clues going through the whole story. Four detected communities can be seen as four relatively independent social cliques. As an example, we go into details of group 4 that is almost separated from the rest of the network. Interestingly, this small social clique consists of 4 parisian students Tholomyes, Listolier, Fameuil and Blacheville with their respective lovers Fantine, Dahlia, Zephine and Favourite. Group 5 consists of 39 outliers, which connect to either two hubs or one of four communities by only a few links. Correspondingly, these outliers are the supporting roles of this novel. Besides this example, more complex structural patterns in real-world networks will be demonstrated and discussed in the rest of this article.

Secondly, such multiple structural patterns may be nested. That is, real-world networks can contain hierarchical organizations with heterogeneous patterns at different levels. In the literature, hierarchical structures are usually studied in a homogeneous way, in which patterns observed in each layer of hierarchies show homophily in terms of either fractal property¹⁸ or modularity in more general cases^{19,20}. A recent study reveals that the patterns demonstrated in each layer of a dendrogram can be assortative (or modular) or disassortative (or bipartite)²¹. The ability to observe heterogeneous patterns at different levels brings new clues for understanding the dynamics of real-world complex networks.

Due to the above two reasons, for an exploratory network about which one often knows little, it is very hard to know what specific structural patterns can be expected and then be obtained by what specific tools. Biased results will be caused if an inappropriate tool is chosen; even if we know something about it beforehand, it is still difficult for a tool exclusively designed for exploring very specific patterns, say modularity, to satisfactorily uncover a multiple of coexisting patterns possibly overlapped or even nested with each other (we call them *multiplex structures* in this work) from networks. To the best of our knowledge, there have been no studies in the literature being able to address both of the above issues. On the other hand, human beings have the capability of simultaneously discovering multiplex and significant structural patterns for various objectives. It has been believed that this kind of capability is an important form of human cognitive and intelligent functions²².

Back to the matrix as shown in the Fig. 1, one would observe an intuitive phenomenon: Any

significant pattern contained in the underlying structures of the network can be statistically highlighted by a group of homogenous individuals with identical or quite similar connectivity profiles. For instance, individuals from the same communities prefer to intensively interact with each other but rarely interact with the rest; hubs would prefer to connect many individuals from different parts of the whole network, whereas all outliers tend to seldom play with others by emitting only a few connections. Based on this naive observation, if one can group the majority of individuals into reasonable clusters according to their connectivity profiles, the coexisting structural patterns can be unveiled by further inferring the linkage among clusters. In this way, the first issue listed above can be promisingly solved.

The idea of grouping nodes into *equivalent* clusters in terms of their connection patterns is quite similar with the philosophy of the *blockmodeling* first proposed by Lorrain and White²³, in which nodes with *structural equivalence* (defined in terms of local neighborhood configurations) or more generally *regular equivalence*²⁴ (defined in terms of globally physical connections to all others) or more softly *stochastic equivalence*^{25,26} (defined in terms of linking probabilities between groups) will be grouped into the same blocks.

Based on the same idea, a very related study has been proposed recently by Newman and Leicht, which first (to our knowledge) shows the motivation to detect unpredefined structural patterns from exploratory networks²⁷. From the perspective of machine learning, their method can be seen as a version of naive Bayes algorithm applied to networks, whose objective is to group nodes with similar connection features into a predefined number of clusters. Although their work only

shows the ability to determine whether an exploratory network is assortative or disassortative by manually analyzing the obtained clusters, it has provided one good proof supporting that the idea of grouping nodes into equivalent clusters can be an initial step of the whole process aiming to unveil multiplex structures from networks.

In this work, we will propose a novel model by introducing the concept of granularity into stochastic connection profiles in order to properly model multiplex structures, and then show how the task of recognizing multiplex structures can be reduced to a simplified version of the isomorphism subgraph matching problem. To test our ideas and strategies proposed here, different sources of networks have been analyzed. It is encouraging that our methods show a good performance, capable of uncovering multiplex structures from the tested networks in a fully automatic way.

2 The Model

Granular couplings We will model the connection profiles of nodes in terms of probabilities instead of physical connectivity. In this way, it is expected not only to find out multiplex structures but also to provide an explicit probabilistic interpretation for these findings within the Bayesian framework. We term such probabilities as *couplings* in that they are not just the mathematical measures subjectively defined for modeling or computing, but they do exist in many real-world systems, encoding different physical meanings such as social preferences in societies, predation habits in ecosystems, co-expression regularities in gene networks or co-occurrence likelihood of

words in languages, which will be valuable to predict their situated systems.

Here the notation of granularity should be interpreted in terms of the resolution and precision. On one hand, in our model we define two kinds of couplings with different resolutions, i.e., *node couplings* and *block couplings*. Formally, we define *node feedforward-coupling* matrix $P_{n \times n}$ and *node feedback-coupling* matrix $Q_{n \times n}$, where p_{ij} and q_{ij} respectively denote the probabilities that node i expects to couple with or to be coupled by node j . In the cases of indirected networks we have $P = Q$ (see SI for proofs). We assume nodes will independently couple with others regulated by such couplings. Nodes with similar feedforward- as well as feedback- coupling distributions will be clustered into the same blocks. In terms of matrices, homogeneous feedforward- and feedback-couplings guarantee homogeneous row and column connection profiles, respectively. Correspondingly, given the block number K , we define *block feedforward-coupling* matrix $\Phi_{K \times K}$ and *block feedback-coupling matrix* $\Psi_{K \times K}$, where ϕ_{pq} and ψ_{pq} respectively denote the probabilities that block C_p expects to couple with or to be coupled by block C_q . We will show later that block couplings can be inferred from node couplings and vice versa. Node couplings with a fine granularity are used to model networks in order to capture their local information as much as possible; while block couplings with a coarser granularity are used to define and recognize global structural patterns by intentionally neglecting trivial details. On the other hand, in the nested patterns, node couplings and block couplings in different hierarchies will have different precisions in order to properly abstract and construct hierarchical organizations. In our model, the couplings on higher layers are the approximations of the related ones on the lower layers. Therefore, as the layers moving from the bottom (corresponding to the original networks) to the top (corresponding to the

finally reduced networks) of the nested organizations, the precision of node or block couplings will gradually degenerate.

Defining multiplex structures The main steps of our strategies for detecting multiplex structures from networks can be stated as follows: 1) simultaneously estimating all kinds of couplings mentioned above and clustering all nodes into nested blocks with a proposed granular blocking algorithm; and 2) in each layer of the nested blocks, recognizing structural patterns by matching predefined isomorphism subgraphs from a reduced blocking model in which trivial couplings are neglected, as illustrated in Fig. 1d. Multiplex structures can be defined in terms of blocks and their couplings. Fig. 2 shows a schematic illustration by means of some conceptual networks. By referring to them, we give following definitions.

A *community* is a self-coupled block. An *authority* is a self-coupled block which is coupled by a number of other blocks. A *hub* is a self-coupled block which couples with a number of other blocks. An *outlier* is a block without self-coupling which is coupled by a hub or couples with an authority. A *bow-tie* is a subgraph consisting of a block b and two sets of blocks $S_l(b)$ and $S_r(b)$, which satisfy with: 1) b is coupled by and couples with the blocks of $S_l(p)$ and $S_r(p)$, respectively; 2) the intersection of $S_l(p)$ and $S_r(p)$ is empty or $\{b\}$; and 3) there are no couplings between $S_l(p)$ and $S_r(p)$; A *multipartite* is a subgraph consisting of a set of blocks without self-couplings which reciprocally couple with each other. As a special case of multipartite, a *bipartite* is a subgraph consisting of two blocks without self-loop couplings which unilaterally or bilaterally coupled with each other. A *hierarchical organization* is a set of nested blocks, in which block subgraphs in

lower layers are directly or indirectly nested in the bigger blocks on higher layers.

The above definitions imply that there may exist overlaps between different patterns in the sense that the same blocks can be simultaneously involved in a multitude of subgraphs. For example, a block which is determined as a community can be also a hub, a authority or the core of one bow tie. Moreover, beyond the predefined patterns, users are allowed to define novel even more complex patterns by designing new subgraphs of blocks, which can be identified by matching their isomorphism counterparts from blocking models.

Granular blocking model Let $N = (V, E)$ be a directed and binary network, where $V(N)$ denotes the set of nodes and $E(N)$ denotes the set of directed links. In the case of undirected network, we suppose there are two direct links between each pair of nodes. Let $A_{n \times n}$ be the adjacency matrix of N , where n is the number of nodes.

Suppose all nodes of N are divided into L ($1 \leq L \leq n$) blocks, denotes by $B_{n \times L}$, where $b_{il} = 1$ if node i is in the block l , otherwise $b_{il} = 0$. When each block is considered to be inseparable, the *granularity* of network N can be measured by the average size of blocks $g = n/L$. As g increasing from 1 to n , the granularity of N degenerates from the finest to the coarsest. Let B_g denote the blocking model with a granularity g , and we expect to cluster all its blocks into a reasonable number of clusters so that the nodes of blocks within the same cluster will demonstrate homogeneous coupling distributions. Let matrix $Z_{L \times K}$ ($1 \leq K \leq L$) denote such clusters, where K is the cluster number and $z_{lk} = 1$ if block l is labeled by cluster k , otherwise $z_{lk} = 0$. Since the coupling distributions of nodes within the same clusters are expected to be homogeneous, one can

characterize such distributions for each cluster instead of for each node. Given Z , define $\Theta_{K \times n}$, where θ_{kj} denotes the probability that any node out of cluster k expects to couple with node v_j ; define $\Delta_{K \times n}$, where δ_{kj} denotes the probability that any node out of cluster k expects to be coupled by node v_j ; define $\Omega = (\omega_1, \dots, \omega_K)^T$, where ω_k denotes the prior probability that a randomly selected node will belong to the cluster C_k . It is easy to show $P = B_g Z \Theta$ and $Q = B_g Z \Delta$ (see SI).

Let $X = (K, Z, \Theta, \Delta, \Omega)$ be a model with respect to N and B_g . We expect to select an optimal X from its hypothesis space to properly fit as well as to precisely predict the behaviors of N under B_g in terms of node couplings characterized by it. According to the MAP principle (maximum a posteriori), the optimal X for a given network N under B_g will be the one with the maximum posterior probability. Moreover, we have: $P(X|N, B_g) \propto P(N|X, B_g)P(X|B_g)$, where $P(X|N, B_g)$, $P(N|X, B_g)$ and $P(X|B_g)$ denote the posteriori of X given N and B_g , the likelihood of N given X and B_g and the priori of X given B_g , respectively.

3 Learning Methods

Likelihood maximization We first consider the simplest case by assuming all the prioris of X given B_g are equal. In this case, we have: $P(X|N, B_g) \propto P(N|X, B_g)$. Let $L(N|X, B_g) = \ln P(N|X, B_g)$, we have (see SI):

$$L(N|X, B_g) = \sum_{l=1}^L \sum_{b_{il} \neq 0} \ln \sum_{k=1}^K \prod_{j=1}^n f(\theta_{kj}, a_{ij}) f(\delta_{kj}, a_{ji}) \omega_k \quad (1)$$

where $f(x, y) = x^y(1 - x)^{1-y}$.

Let $L(N, Z|X, B_g)$ be the log-likelihood of the joint distribution of N and Z given X and B_g , we have (see SI):

$$L(N, Z|X, B_g) = \sum_{l=1}^L \sum_{b_{il} \neq 0} \sum_{k=1}^K z_{lk} \left(\sum_{j=1}^n (\ln f(\theta_{kj}, a_{ij}) + \ln f(\delta_{kj}, a_{ji})) + \ln \omega_k \right) \quad (2)$$

Considering the expectation of $L(N, Z|X, B_g)$ on Z , we have:

$$E[L(N, Z|X, B_g)] = \sum_{l=1}^L \sum_{b_{il} \neq 0} \sum_{k=1}^K \gamma_{lk} \left(\sum_{j=1}^n (\ln f(\theta_{kj}, a_{ij}) + \ln f(\delta_{kj}, a_{ji})) + \ln \omega_k \right) \quad (3)$$

where $E[z_{lk}] = \gamma_{lk} = P(y = k|b = l, X, B_g)$, i.e., the probability that block l will be labeled as cluster k given X and B_g .

Let $J = E[L(N, Z|X, B_g)] + \lambda(\sum_{k=1}^K \omega_k - 1)$ be a Lagrangian function constructed for

maximizing $E[L(N, Z|X, B_g)]$ with a constraint $\sum_{k=1}^K \omega_k = 1$, we have:

$$\begin{cases} \frac{\partial J}{\partial \theta_{kj}} = 0 \\ \frac{\partial J}{\partial \delta_{kj}} = 0 \\ \frac{\partial J}{\partial \omega_k} = 0 \\ \frac{\partial J}{\partial \lambda} = 0 \end{cases} \Rightarrow \begin{cases} \theta_{kj} = \frac{\sum_{l=1}^L \sum_{b_{il} \neq 0} a_{ij} \gamma_{lk}}{\sum_{l=1}^L \sum_{b_{il} \neq 0} \gamma_{lk}} \\ \delta_{kj} = \frac{\sum_{l=1}^L \sum_{b_{il} \neq 0} a_{ji} \gamma_{lk}}{\sum_{l=1}^L \sum_{b_{il} \neq 0} \gamma_{lk}} \\ \omega_k = \frac{\sum_{l=1}^L \sum_{b_{il} \neq 0} \gamma_{bk}}{n} \end{cases} \quad (4)$$

According to the Bayesian theorem, we have (see SI):

$$\gamma_{lk} = \frac{1}{\sum_{i=1}^n b_{il}} \sum_{b_{il} \neq 0} \frac{\prod_{j=1}^n f(\theta_{kj}, a_{ij}) f(\delta_{kj}, a_{ji}) \omega_k}{\sum_{k=1}^K \prod_{j=1}^n f(\theta_{kj}, a_{ij}) f(\delta_{kj}, a_{ji}) \omega_k} \quad (5)$$

Using the similar treatment as proposed by Dempster and Laird²⁸, we can prove that a local optimum of Eq.10 will be guaranteed by recursively calculating Eqs.4 and 12 (see SI). The time complexity of this iterative computing process is $O(In^2K)$, where I is the iterations required for convergence, which is usually quite small. An approximate but much faster version with a time $O(ILnK)$ is given in the SI.

Priori approximation Without considering the priori of the model, the above-proposed likelihood maximization algorithm will be cursed by the overfitting problem. That is, $L(N|X, B_g)$ will monotonically increase as K approaching to L . In this section, we will discuss how to approximately estimate the prior $P(X|B_g)$ by means of the information theory.

Note that $1 \leq K \leq L = n/g$, which implies that the coarser granularity the smaller K . It will be shown in the following that a smaller K will indicate a less complexity of X . So, we have: a coarser granularity prefer simpler models, which can be mathematically written as $P(X|B_g) =$

$\eta(X)^g$, where the function $\eta(X)$ measures the complexity of X in terms of its parameters. In this work, we set $\eta(X) = P(X|B_1) = P(X)$, where $P(X)$ is the priori of X in the hypothesis space in which K can be freely valued from 1 to n . According to Shannon and Weaver²⁹, $\ln(1/P(X))$ is the minimum description length of X with a prior $P(X)$ in its model space. Let $OC(X)$ denote the optimal coding schema for X , and let $L_{OC}(X)$ be the minimum description length of X under this schema. We have: $-\ln P(X|B_g) = -g \ln P(X) = gL_{OC}(X)$. Now, to estimate the prior $P(X|B_g)$ is to design a good coding (or compressing) schema as close to OC as possible.

In terms of the parameter of X , i.e., Θ , Δ , Z and Ω , we have (see SI):

$$\Phi = \Theta B_g Z D^{-1}, \quad \Psi = \Delta B_g Z D^{-1} \quad (6)$$

where $D = \text{diag}(n\Omega)$.

Note that matrices Z and B_g can be compressed into a map y , where $y(i) = k$ if the entry (i, k) of $B_g Z$ is equal to one. Given y , Φ and Ψ , node couplings p_{ij} and q_{ij} can be measured by:

$$p_{ij} = \phi_{y(i), y(j)}, \quad q_{ij} = \psi_{y(i), y(j)} \quad (7)$$

Eq.7 says that, all node couplings can be approximately characterized by y , Φ and Ψ . In other word, the compressing schema close to $OC(X)$ we have found out is:

$$\widehat{OC}(X) = (K, \Phi_{K \times K}, \Psi_{K \times K}, y_{n \times 2}) \quad (8)$$

Now, we have,

$$\begin{aligned}
L_{\widehat{OC}}(X) &= 1 \times \left(-\ln \frac{1}{1}\right) + 2K^2 \left(-\ln \frac{1}{K^2}\right) + 2n \left(-\ln \frac{1}{2n}\right) \\
&= 2K^2 \ln K^2 + 2n \ln 2n
\end{aligned}$$

Moreover, we have:

$$\begin{aligned}
&\arg \max_X P(X|N, B_g) \\
&= \arg \min_X (-\ln P(N|X, B_g) - \ln P(X|B_g)) \\
&= \arg \min_X (-\ln P(N|X, B_g) + gL_{\widehat{OC}}(X)) \tag{9} \\
&= \arg \min_X (-L(N|X, B_g) + g(2K^2 \ln K^2 + 2n \ln 2n)) \\
&= \arg \min_X (-L(N|X, B_g) + 2gK^2 \ln K^2)
\end{aligned}$$

Eq.9 tries to seek a good tradeoff between the accuracy of model (or the precision of fitting observed data) measured by the likelihood of a network, and the complexity of a model (or the generalization ability to predict new data) measured by its optimal coding length.

Model selection For a given K , the penalty term is a constant, and thus to maximize $P(X|N, B_g)$ is to maximize $L(N|X, B_g)$. In our algorithm, K will be systematically checked from 1 to L , and the model with the minimum sum of negative likelihood and penalty will be returned as the optimal one. In the landscape of K and $P(X|N, B_g)$, a well-like curve will be shaped during the whole search process (see SI). So, in practice, rather than mechanically checking K for exact L times, an ongoing searching can be stopped after it has safely passed the well bottom. By means of this greedy strategy, the efficiency of our algorithm would be greatly improved. The complete

algorithm is given in the SI.

Hierarchy construction Assume we have constructed h layers, in which the $i - th$ layer corresponds to a blocking model characterized by B_{g_i} . Now, we want to construct the $(h + 1) - th$ layer by selecting an X with a maximum posterior given a set of blocking models on different layers. We have shown that (see SI): $P(X|N, B_{g_1}, \dots, B_{g_h}) \propto P(N|X, B_{g_h})P(X|B_{g_h}) \propto P(N|X, B_{g_h})P(X)^{g_h}$. This Markov-like process indicates that the new model to be selected for layer h is only based on the information of the layer $h - 1$. So, for a given network, its hierarchical organization can be incrementally constructed as follows.

Firstly, we construct the first layer by taking each node as one block, and cluster it into K_1 clusters by selecting an model with a maximum $P(X|N, B_1)$. Next, we form B_{n/K_1} by capsuling each cluster on the first layer as one block, and cluster these blocks into K_2 clusters by selecting an new model with a maximum $P(X|N, B_{n/K_1})$, which forms the second layer. We repeat the same procedure until it converges (the cluster number obtained keeps fixed). In this way, the number of layers of a hierarchical organization will be automatically determined. The above procedure can be seen as a semi-supervised learning process; in the cases that the granularity is more than one, we have already known a priori that which nodes will be definitely within the same clusters. As the layer in the constructed hierarchy increases, the homogeneity of the nodes within the same cluster in terms of their connection profiles keeps degenerating, and correspondingly more global patterns are allowed to be observed by tolerating such increasing diversities.

Isomorphism subgraph matching Based on the obtained blocks in the level $h + 1$ of the hierarchy, all potential patterns hidden in the level h can be revealed through an isomorphism subgraph matching procedure, whose input is the block feedforward-coupling matrix Φ . First we construct a reduced blocking model by taking each block as one node, and for each pair of blocks p and q we insert a link from p to q if ϕ_{pq} is above a threshold computed based on Φ (see SI). Then for each block, we pick up the matched isomorphism subgraphs it will be involved in, and put them into categorized reservoirs labeled by different patterns. During this procedure, the subgraph to be put into a reservoir will be discarded if it is a subgraph of an existing one, as illustrated by Fig.3d.

4 Applications

Exploring the cash flow patterns of the world trade system The discovered multiplex structures as well as their granular couplings can be used to understand some dynamics of networks. Here we give one example to show how cash possibly flow through a world trade net. Fig. 3a shows a directed network encoding the trade relationship among eighty countries in the world in 1994, which was originally constructed by Nooy³⁰ based on the commodity trade statistics published by the United Nations. Nodes denote countries, and each arc $i \rightarrow j$ denotes the country i imported high technology products or heavy manufactures from the country j . Analogous to the "structural world system positions" initially suggested by Smith and White based on their analysis of the international trade from 1965 to 1980³¹, the eighty countries in 1994 were categorized into three classes according to their economic roles in the world: core, semi-periphery and periphery³⁰. Accordingly, in the visualized network, the countries labeled by them are distributed along three

circles from inside to outside, respectively.

A two-layer hierarchical organization has been constructed by our system, as illustrated in Fig. 3d. A reduced blocking model is shown in the first layer by neglecting trivial couplings, in which six blocks are obtained. By referring the matrix of the network as presented in Fig. 3b, one can observe that the nodes within the same blocks demonstrate homogeneous row as well as column connection profiles. By referring to their couplings, ten isomorphism subgraphs of the patterns as defined in Fig. 2 are recognized, which, respectively, are one authority, four communities, three hubs and two outliers, as shown in Fig. 3e. Quite a few interesting things can be read from these uncovered multiplex structures. Globally, the countries near center tend to have larger out-degrees, while those far from center have smaller even zero out-degrees. Specifically, (1) according to the coupling strength from strong to weak, three detected hubs can be ranked into the sequence of blocks 4, 1 and 3. The first two hubs consist of the "core" of the trade system except for Spain and Denmark; (2) the countries from blocks 3, 2 and 6 consist of the backbone of the "semi-periphery"; (3) more than a half of "periphery" countries (10 of 17) have zero out-degrees; (4) interestingly, the detected blocks are also geography-related, as illustrated in Fig. 3c. Most countries of hubs 4 and 1 are from western Europe except America, China and Japan; most of hub 3 are from southeastern Asia; most of the community block 6 are from north or south America; most of the outlier block 2 are from eastern Europe; most of the outlier block 5 are from Africa or some areas of Asia.

In the second layer, a macroscopic hub-outlier pattern with strong couplings is recognized.

Hub blocks 4 and 1 in the first layer collectively form a more global hub of the whole network as the core of the entire trade system; other blocks form a more global outlier of the network corresponding to the semi-periphery and periphery of the trade system. This nested hub-outlier patterns perhaps give us an evidence about how cash flowed through the world in different levels in 1994. Note that arc $i \rightarrow j$ denotes that country i imported commodities from country j , which also indicates that the spent cash has flowed from i to j . In this way, one can image cash flows along these arcs from one country to another. According to the global pattern in the second layer, the dominant cash flux will flow from the core countries to themselves with a probability 0.6, and to the rest with a probability 0.57. Locally, the blocking model in the first layer shows the backbone of the cash flow through the entire world with their respective strength in terms of block couplings, as illustrated in Fig. 3d.

Mining granular association rules from networks When a network encodes the co-occurrence of events, its underlying node- or block-coupling matrices would imply the probabilistic associations among these events in different granular levels, respectively. Formally, we have: *node association rule (NAR)*: $i \rightarrow j \langle p_{ij} \rangle$, and *block association rule (BAR)*: $B_p \rightarrow B_q \langle \phi_{pq} \rangle$. A *NAR* means that event j would happen with a probability p_{ij} given event i happens. A *BAR* means that any event of block q would happen with a probability ϕ_{pq} given any event of block p happens. Such association rules with different granularities can be used in making prediction in a wide range of applications, such as online recommender systems. We will demonstrate this idea with a political book co-purchasing network compiled by V. Krebs, as given in Fig. 4(a), where nodes represent books about US politics sold by the online bookseller Amazon.com, and edges connects pairs of

books that are frequently co-purchased, as indicated by the "customers who bought this book also bought these other books" feature on Amazon. Moreover, these books have been labeled as "liberal", "neutral" or "conservative" according to their stated or apparent political alignments based on the descriptions and reviews of the books posted on Amazon.com ³².

A two-layer hierarchical organization has been detected by our system as shown in Fig. 4. The blocking model of the first layer is shown in Fig. 4(b). By matching isomorphism subgraphs in its reduced blocking model, nine patterns are recognized, which respectively are five communities (blocks 1,2,4,6,7), two cores (blocks 2 and 7), two outliers (blocks 3 and 5) and a bow tie (blocks 1,2,3). Note that, in indirected networks, the core of a bow tie (block 2 in this case) can be seen as the overlapping part of its two wings (blocks 1 and 3 in this case) by neglecting the direction of links. In the second layer, a macroscopic community structure is recognized, as shown in Fig. 4(c). Interestingly, the left and right communities can be globally labeled as "left-wing" and "right-wing" according to the types of the books they contain respectively. Such a global pattern can be seen as one macroscopic *BAR*: the books with common labels would be co-purchased with a great chance (about 15%); while, those with different labels are rarely co-purchased (only with a chance of 1%).

When zooming in to both global communities in the second layer, one will obtain 7×7 mesoscopic *BARs* encoded by the block-coupling matrix Φ , as illustrated by the weighted arrow lines Fig. 4(b). As an example, we list the *BRAs* related to the block 2 in a decreasing sequence of association strength. $B_2 \rightarrow B_2 \langle 0.60 \rangle$; $B_2 \rightarrow B_3 \langle 0.44 \rangle$; $B_2 \rightarrow B_1 \langle 0.21 \rangle$; $B_2 \rightarrow B_4 \langle 0.06 \rangle$;

$B_2 \rightarrow B_6\langle 0.04 \rangle$; $B_2 \rightarrow B_5\langle 0 \rangle$; $B_2 \rightarrow B_7\langle 0 \rangle$. Such mesoscopic association rules would help booksellers adaptively adjust their selling strategies to determine what kinds of stocks they should increase or decrease based on the statistics of past sales. For example, if they find the books labeled as block 2 are sold well, they may correspondingly increase the order of books labeled as blocks 1 and 3 besides block 2, while they may simultaneously decrease the order of books labeled as blocks 5 or 7.

More specifically, with the aid of NARs, booksellers would be able to estimate the chance that customers will spend their money on a book j if they have already bought book i by referring to $i \rightarrow j\langle p_{ij} \rangle$. Such microscopic rules would provide booksellers the suggestions on what specific books should be listed according to what sequence in the recommending area of the web page advertising a book. For example, for the book "*The Price of Loyalty*", the most worth recommended books are listed as follows according to the coupling strength to it: *Big Lies* $\langle 0.91 \rangle$; *Bushwhacked* $\langle 0.73 \rangle$; *Plan of Attack* $\langle 0.73 \rangle$; *The Politics of Truth* $\langle 0.73 \rangle$; *The Lies of George W.Bush* $\langle 0.73 \rangle$; *American Dynasty* $\langle 0.64 \rangle$; *Bushwomen* $\langle 0.64 \rangle$; *The Great Unraveling* $\langle 0.64 \rangle$; *Worse Than Watergate* $\langle 0.64 \rangle$.

5 Conclusions

In this work, we have shown through examples that the structural patterns coexisting in the same real-world complex network can be miscellaneous, overlapped or nested, which collaboratively shape a heterogeneous hierarchical organization. We have proposed a framework based on the concept of granular couplings and the proposed granular blocking model to uncover such multi-

plex structures from networks. From the output of patterns, hierarchies and granular couplings generated by our approach, one can analyze or even predict some dynamics of networks, which are helpful for both theoretical studies and practical applications.

Moreover, based on the rationale behind this work, we suggest that the evolution of a real-world network may be driven by the co-evolution of its structural patterns and its underlying couplings. On one hand, statistically significant patterns would be gradually highlighted and emergently shaped by the aggregations of homogeneous individuals in terms of their couplings. On the other hand, individuals would adaptively adjust their respective couplings according to the currently evolved structural patterns.

References

1. Boccaletti S, Latora V, Moreno Y, Chavez M, Hwang DU(2006) Complex networks: Structure and dynamics. *Physics Reprints* 424:175-308.
2. Milo R, Orr SS, Itzkovitz S, Kashtan N, Chklovskii D, Alon U(2002) Network Motifs: simple building blocks of complex networks. *Science* 298:824-827.
3. Girvan M, Newman MEJ(2002) Community structure in social and biological networks. *Proc Natl Acad Sci USA* 99:7821-7826.
4. Watts DJ, Strogatz SH(1998) Collective Dynamics of Small-World Networks. *Nature* 393:440-442.

5. Barabasi AL, Albert R(1999) Emergence of Scaling in Random Networks. *Science* 286:509-512.
6. Fortunato S(2010) Community detection in graphs. *Physics Reports* 486:75-174.
7. Holme P, Liljeros F, Edling CR, Kim BJ(2003) Network bipartivity. *Phys Rev E* 68:056107.
8. Guillaume JL, Latapy M(2004) Bipartite structure of all complex networks. *Inform Process Lett* 90:215-221.
9. Brady A, Maxwell K, Daniels N, Cowen LJ(2009) Fault Tolerance in Protein Interaction Networks: Stable Bipartite Subgraphs and Redundant Pathways. *PLoS ONE* 4:e5364.
10. Kleinberg JM(1999) Authoritative Sources in a Hyperlinked Environment. *Journal of ACM* 46:604-632.
11. Albert R, Jeong H, Barabasi AL(2000) The Internet's Achilles heel: Error and attack tolerance of complex networks. *Nature* 406:378-382.
12. Sporns O, Honey C, Kotter R(2007) Identification and classification of hubs in brain networks. *PLoS ONE* 2:e1049.
13. Broder A, Kumar R, Maghoul F, Raghavan P, Rajagopalan S, Stata R, Tomkins A, Wiener J(1999) Graph structure in the Web. *COMPUT NETW* 33:309-320.
14. News Feature(2000) The web is a bow tie. *Nature* 405:113.
15. Ma HW, Zeng AP(2003) The connectivity structure, giant strong component and centrality of metabolic networks. *Bioinformatics* 19:1423-1430.

16. Palla G, Derenyi I, Farkas I, Vicsek T(2005) Uncovering the overlapping community structures of complex networks in nature and society. *Nature* 435:814-818.
17. Knuth DE(1993). *The Stanford GraphBase: A Platform for Combinatorial Computing* (Addison-Wesley press, Reading, MA).
18. Ravasz E, Somera AL, Mongru DA, Oltvai ZN, Barabasi AL(2002) Hierarchical organization of modularity in metabolic networks. *Science* 297:1551-1555.
19. Zhou C, Zemanova L, Zamora G, Hilgetag CC, Kurths J(2006) Hierarchical Organization Unveiled by Functional Connectivity in Complex Brain Networks. *Phys Rev Lett* 97:238103.
20. Pardo MS, Guimera R, Moreira AA, Amaral LAN(2007) Extracting the hierarchical organization of complex systems. *Proc Natl Acad Sci USA* 104:7821-7826.
21. Clauset A, Moore C, Newman MEJ(2008) Hierarchical structure and the prediction of missing links in networks. *Nature* 453:98-101.
22. kemp C, Tenenbaum JB(2008) The discovery of structural form. *Proc Natl Acad Sci USA* 105:10687-10692.
23. Lorrain F, White HC(1971) Structural equivalence of individuals in social networks. *J MATH SOCIOLOG* 1:49-80.
24. White DR, Reitz KP(1983) Graph and semigroup homomorphism on networks of relations. *Social Networks* 5:193-235.

25. Fienberg SE, Wasserman S(1981) Categorical data analysis of single sociometric relations. *Sociological methodology* 12:156-192.
26. Holland PW, Laskey KB, Leinhardt S(1983) Stochastic blockmodels: Some first steps. *Social Networks* 5:109-137.
27. Newman MEJ, Leicht EA(2007) Mixture models and exploratory analysis in networks. *Proc Natl Acad Sci USA* 104:9564-9569.
28. Dempster AP, Laird NM, Rubin DB(1977) Maximum likelihood from incomplete data via the EM algorithm. *J R Statist Soc B* 39:185-197.
29. Shannon CE, Weaver W(1949) *The mathematical theory of communication* (University of Illinois Press, Urbana).
30. Nooy WD, Mirvar A, Batagelj V(2004) *Exploratory social network analysis with Pajek* (Cambridge University Press)
31. Smith DA, White DR(1992) Structure and Dynamics of the Global Economy - Network Analysis of International-Trade 1965-1980. *Social Forces* 70:857-893.
32. Newman MEJ(2006) Finding community structure in networks using the eigenvectors of matrices. *Phys Rev E* 74:036104.

Support Information

A Proofs and algorithms

Proposition 1. *For an indirected network, its feedforward-coupling matrix P is equal to its feedback-coupling matrix Q .*

Proof.

$$\begin{aligned} p_{ij} &= P(i \rightarrow j | y = k) \\ &= \sum_{k=1}^K m_{ik} P(i \rightarrow j | y = k) \\ &= \sum_{k=1}^K (\sum_{l=1}^L b_{il} z_{lk}) P(i \rightarrow j | y = k) \\ &= \sum_{l=1}^L \sum_{k=1}^K b_{il} z_{lk} \theta_{kj} \end{aligned}$$

where $i \rightarrow j$ denote the event that node v_i couples with v_j , and $y = k$ denote the event that v_i is labeled by cluster k ; $m_{ik} = 1$ if v_i is labeled by cluster k , otherwise $m_{ik} = 0$. So we have

$$P = B_g Z \Theta.$$

$$\begin{aligned} q_{ij} &= P(i \leftarrow j | y = k) \\ &= \sum_{k=1}^K m_{ik} P(i \leftarrow j | y = k) \end{aligned}$$

$$= \sum_{k=1}^K (\sum_{l=1}^L b_{il} z_{lk}) P(i \leftarrow\!\!\!\rightarrow j | y = k)$$

$$= \sum_{l=1}^L \sum_{k=1}^K b_{il} z_{lk} \delta_{kj}$$

where $i \leftarrow\!\!\!\rightarrow j$ denote the event that node v_i except to be coupled by v_j . So we have

$$Q = B_g Z \Delta.$$

If A is symmetry, from the Eq.4 in the article, we have

$$\theta_{kj} = \frac{\sum_{l=1}^L \sum_{b_{il} \neq 0} a_{ij} \gamma_{lk}}{\sum_{l=1}^L \sum_{b_{il} \neq 0} \gamma_{lk}} = \frac{\sum_{l=1}^L \sum_{b_{il} \neq 0} a_{ji} \gamma_{lk}}{\sum_{l=1}^L \sum_{b_{il} \neq 0} \gamma_{lk}} = \delta_{kj}.$$

So we have $P = Q$. □

Proposition 2.

$$L(N|X, B_g) = \sum_{l=1}^L \sum_{b_{il} \neq 0} \ln \sum_{k=1}^K \Pi_{j=1}^n f(\theta_{kj}, a_{ij}) f(\delta_{kj}, a_{ji}) \omega_k \quad (10)$$

where $f(x, y) = x^y (1 - x)^{1-y}$.

Proof. Let $v = i$ denote the event that a node with linkage structure $\langle a_{i1}, \dots, a_{in}, a_{1i}, \dots, a_{ni} \rangle$ will be observed in network N . Let $y = k$ denote the event that the cluster label assigned to a node is equal to k . Let $i \rightarrow_{a_{ij}} j$ denote the event that node v_i link to node v_j or not depending on a_{ij} . Let $i \leftarrow_{a_{ji}} j$ denote the event that node v_i will be linked by node v_j or not depending on a_{ji} . We have:

$$L(N|X, B_g) = \ln \Pi_{i=1}^n P(v = i) = \sum_{i=1}^n \ln P(v = i)$$

$$\begin{aligned}
&= \sum_{i=1}^n \ln P((v = i) \cap (\cup_{k=1}^K y = k)) \\
&= \sum_{i=1}^n \ln \sum_{k=1}^K P(v = i, y = k) \\
&= \sum_{i=1}^n \ln \sum_{k=1}^K (P(v = i|y = k)P(y = k)) \\
&= \sum_{i=1}^n \ln \sum_{k=1}^K (P(< a_{i1}, \dots, a_{in}, a_{1i}, \dots, a_{ni} > |y = k)P(y = k)) \\
&= \sum_{i=1}^n \ln \sum_{k=1}^K (\Pi_{j=1}^n P(i \rightarrow_{a_{ij}} j|y = k)P(i \leftarrow_{a_{ji}} j|y = k)P(y = k)) \\
&= \sum_{i=1}^n \ln \sum_{k=1}^K (\Pi_{j=1}^n (\theta_{kj}^{a_{ij}} (1 - \theta_{kj})^{1-a_{ij}})(\delta_{kj}^{a_{ji}} (1 - \delta_{kj})^{1-a_{ji}})\omega_k) \\
&= \sum_{i=1}^n \ln \sum_{k=1}^K (\Pi_{j=1}^n f(\theta_{kj}, a_{ij})f(\delta_{kj}, a_{ji})\omega_k) \\
&= \sum_{l=1}^L \sum_{b_{il} \neq 0} \ln \sum_{k=1}^K (\Pi_{j=1}^n f(\theta_{kj}, a_{ij})f(\delta_{kj}, a_{ji})\omega_k) \quad \square
\end{aligned}$$

Proposition 3.

$$L(N, Z|X, B_g) = \sum_{l=1}^L \sum_{b_{il} \neq 0} \sum_{k=1}^K z_{lk} \left(\sum_{j=1}^n (\ln f(\theta_{kj}, a_{ij}) + \ln f(\delta_{kj}, a_{ji})) + \ln \omega_k \right) \quad (11)$$

Proof. Let $y(i)$ denote the cluster label assigned to node i under the given partition Z , we have:

$$\begin{aligned}
&L(N, Z|X, B_g) \\
&= \ln \Pi_{i=1}^n P(v = i, y = y(i)) \\
&= \sum_{i=1}^n \ln \sum_{k=1}^K m_{ik} P(v = i, y = k)
\end{aligned}$$

$$\begin{aligned}
&= \sum_{i=1}^n \ln \sum_{k=1}^K m_{ik} P(v = i|y = k) P(y = k) \\
&= \sum_{i=1}^n \sum_{k=1}^K \ln(P(v = i|y = k) P(y = k))^{m_{ik}} \\
&= \sum_{i=1}^n \sum_{k=1}^K m_{ik} \ln(P(v = i|y = k) P(y = k)) \\
&= \sum_{i=1}^n \sum_{k=1}^K m_{ik} \ln(\Pi_{j=1}^n (\theta_{kj}^{a_{ij}} (1 - \theta_{kj}^{1-a_{ij}}) \delta_{kj}^{a_{ji}} (1 - \delta_{kj}^{1-a_{ji}})) \omega_k) \\
&= \sum_{i=1}^n \sum_{k=1}^K m_{ik} (\sum_{j=1}^n (\ln f(\theta_{kj}, a_{ij}) + \ln f(\delta_{kj}, a_{ji})) + \ln \omega_k) \\
&= \sum_{b_{i1} \neq 0} \sum_{k=1}^K z_{1k} (\sum_{j=1}^n (\ln f(\theta_{kj}, a_{ij}) + \ln f(\delta_{kj}, a_{ji})) + \ln \omega_k) + \dots \\
&\quad + \sum_{b_{iL} \neq 0} \sum_{k=1}^K z_{Lk} (\sum_{j=1}^n (\ln f(\theta_{kj}, a_{ij}) + \ln f(\delta_{kj}, a_{ji})) + \ln \omega_k) \\
&= \sum_{l=1}^L \sum_{b_{il} \neq 0} \sum_{k=1}^K z_{lk} (\sum_{j=1}^n (\ln f(\theta_{kj}, a_{ij}) + \ln f(\delta_{kj}, a_{ji})) + \ln \omega_k).
\end{aligned}$$

□

Notice that, in the proofs of Props 2 and 3, all probabilities such as $P(y = k|v = i)$ and $P(y = k)$ are discussed under the conditions of X and B_g . To simplify the equations, we omit them without losing correctness.

Proposition 4.

$$\gamma_{lk} = \frac{1}{\sum_{i=1}^n b_{il}} \sum_{b_{il} \neq 0} \frac{\Pi_{j=1}^n f(\theta_{kj}, a_{ij}) f(\delta_{kj}, a_{ji}) \omega_k}{\sum_{k=1}^K \Pi_{j=1}^n f(\theta_{kj}, a_{ij}) f(\delta_{kj}, a_{ji}) \omega_k} \quad (12)$$

Proof. let $P(y = k|v = i)$ be the probability that node i belongs to cluster k given X and B_g . We have:

$$\gamma_{lk} = P(y = k|b = l, X, B_g) = \sum_{b_{il} \neq 0} \frac{1}{\sum_{i=1}^n b_{il}} P(y = k|v = i)$$

where $\frac{1}{\sum_{i=1}^n b_{il}}$ is the probability of selecting node i from block l .

According to the Bayesian theorem, we have:

$$P(y = k|v = i) = \frac{P(y=k)P(v=i|y=k)}{\sum_{k=1}^K P(y=k)P(v=i|y=k)}.$$

Based on the proof of Prop.2, we have:

$$P(y = k)P(v = i|y = k) = \prod_{j=1}^n f(\theta_{kj}, a_{ij})f(\delta_{kj}, a_{ji})\omega_k.$$

So, we have Eq.12. □

As an approximate version of Eq.12, we have:

$$\begin{aligned} \gamma_{lk} &= P(y = k|b = l) = P(y = k|v = i, b_{il} \neq 0) \\ &= \frac{P(y = k)P(v = i, b_{il} \neq 0|y = k)}{\sum_{k=1}^K P(y = k)P(v = i, b_{il} \neq 0|y = k)} \\ &= \frac{\exists_{b_{il} \neq 0} \prod_{j=1}^n f(\theta_{kj}, a_{ij})f(\delta_{kj}, a_{ji})\omega_k}{\sum_{k=1}^K \exists_{b_{il} \neq 0} \prod_{j=1}^n f(\theta_{kj}, a_{ij})f(\delta_{kj}, a_{ji})\omega_k} \end{aligned} \tag{13}$$

where $\exists_{b_{il} \neq 0}$ denotes that randomly selecting a node from block l .

That is, instead of averaging all nodes in the block l , the real value of γ_{lk} can be approximately estimated by a randomly selected node from block l .

Correspondingly, an approximate version of the log-likelihood of Eq.10 is given by:

$$L(N|X, B_g) = \sum_{l=1}^L N_l (\exists_{b_{il} \neq 0} \ln \sum_{k=1}^K \prod_{j=1}^n f(\theta_{kj}, a_{ij}) f(\delta_{kj}, a_{ji}) \omega_k) \quad (14)$$

where N_l denotes the size of block l .

The time calculating Eqs.12 and 10 will be bounded by $O(n^2K)$. While, the time calculating Eqs.13 and 14 will be bounded by $O(LnK)$. This will be much efficient for constructing the hierarchical organizations of networks.

Theorem 1. *A local optimum of Eq.10 will be guaranteed by recursively calculating Eqs.4 and 5 in the article.*

Proof. From the Proposition2, we have:

$$\begin{aligned} L(N|X, B_g) &= \sum_{i=1}^n \ln P(v = i|X, B_g) \\ &= \sum_{i=1}^n \ln \sum_{k=1}^K P(v = i, y = k|X, B_g) \\ &= \sum_{i=1}^n \ln \sum_{k=1}^K P(y = k|v = i, X^{(s)}, B_g) \frac{P(v=i, y=k|X, B_g)}{P(y=k|v=i, X^{(s)}, B_g)} \end{aligned}$$

(by Jensen's inequality)

$$\geq \sum_{i=1}^n \sum_{k=1}^K P(y = k|v = i, X^{(s)}, B_g) \ln \frac{P(v=i, y=k|X, B_g)}{P(y=k|v=i, X^{(s)}, B_g)}$$

$$\equiv G(X, X^{(s)}).$$

Furthermore, we have:

$$G(X^{(s)}, X^{(s)})$$

$$= \sum_{i=1}^n \sum_{k=1}^K P(y = k|v = i, X^{(s)}, B_g) \ln \frac{P(v=i, y=k|X^{(s)}, B_g)}{P(y=k|v=i, X^{(s)}, B_g)}$$

$$= \sum_{i=1}^n \sum_{k=1}^K P(y = k|v = i, X^{(s)}, B_g) \ln P(v = i|X^{(s)}, B_g)$$

$$= \sum_{i=1}^n \ln P(v = i|X^{(s)}, B_g) \sum_{k=1}^K P(y = k|v = i, X^{(s)}, B_g)$$

$$= \sum_{i=1}^n \ln P(v = i|X^{(s)}, B_g)$$

$$= L(N|X^{(s)}, B_g).$$

Let $P(y = k|b = l, X^{(s)}, B_g) = \gamma_{lk}^{(s)}$, we have:

$$G(X, X^{(s)})$$

$$= \sum_{l=1}^L \sum_{b_{il} \neq 0} \sum_{k=1}^K \gamma_{lk}^{(s)} \ln P(v = i, y = k|X, B_g) - \sum_{l=1}^L \sum_{b_{il} \neq 0} \sum_{k=1}^K \gamma_{lk}^{(s)} \ln P(y = k|v = i, X^{(s)}, B_g).$$

So, we have:

$$\arg \max G(X, X^{(s)})$$

$$= \arg \max (\sum_{l=1}^L \sum_{b_{il} \neq 0} \sum_{k=1}^K \gamma_{lk}^{(s)} \ln P(v = i, y = k | X, B_g) - \sum_{l=1}^L \sum_{b_{il} \neq 0} \sum_{k=1}^K \gamma_{lk}^{(s)} \ln P(y = k | v = i, X^{(s)}, B_g))$$

$$= \arg \max (\sum_{l=1}^L \sum_{b_{il} \neq 0} \sum_{k=1}^K (\gamma_{lk}^{(s)} \ln P(v = i, y = k | X, B_g)))$$

$$= \arg \max E[L(N, Z^{(s)} | X, B_g)]$$

$$= X^{(s+1)}.$$

Recall that, the $\Theta^{(s+1)}$, $\Delta^{(s+1)}$ and $\Omega^{(s+1)}$ of $X^{(s+1)}$ can be computed in terms of $\gamma_{lk}^{(s)}$ by Eq.4 in the article. So, we have:

$$G(X^{(s+1)}, X^{(s)}) \geq G(X^{(s)}, X^{(s)}) = L(N | X^{(s)}, B_g).$$

Recall that $L(N | X, B_g) \geq G(X, X^{(s)})$, we have:

$$L(N | X^{(s+1)}, B_g) \geq G(X^{(s+1)}, X^{(s)}) \geq G(X^{(s)}, X^{(s)}) = L(N | X^{(s)}, B_g).$$

That is to say, the $X^{(s+1)}$ obtained in the current iteration will be not worse than $X^{(s)}$ obtained in last iteration. So, we have the theorem. □

Proposition 5. *In terms of the parameter of X , Θ , Δ , Z and Ω , we have:*

$$\Phi = \Theta B_g Z D^{-1}, \quad \Psi = \Delta B_g Z D^{-1} \tag{15}$$

where $D = \text{diag}(n\Omega)$.

Proof. We have

$$\phi_{pq} = \sum_{i \in C_q} \frac{1}{N_q} \theta_{pi}$$

where $i \in C_q$ denotes node i is in the cluster q with a size N_q , and $\frac{1}{N_q}$ is the probability of selecting node i from cluster q . Furthermore, we have:

$$\phi_{pq} = \frac{1}{n\omega_q} \sum_{i=1}^n \theta_{pi}(B_g Z)_{iq}.$$

Similarly, we have:

$$\psi_{pq} = \frac{1}{n\omega_q} \sum_{i=1}^n \delta_{pi}(B_g Z)_{iq}.$$

So, we have

$$\Phi = \Theta B_g Z D^{-1}, \quad \Psi = \Delta B_g Z D^{-1}.$$

□

Algorithm 1. *Searching the optimal model X given N and B_g*

$$X = GBM(N, B_g)$$

$$01. \quad K = 1;$$

$$02. \quad X^{(0)} = LM(N, K, B_g); L^{(0)} = -\ln(N|X^{(0)}, B_g);$$

$$03. \quad \text{for } K=2:n$$

$$04. \quad X^{(1)} = LM(N, K, B_g);$$

```

05.       $L^{(1)} = -\ln(N|X^{(1)}, B_g) + 2gK^2 \ln K^2;$ 

06.      if  $L^{(1)} < L^{(0)}$  then

07.           $X^{(0)} = X^{(1)}; L^{(0)} = L^{(1)};$ 

08.      endif

09.      if  $L^{(1)}$  keeps increasing for predefined steps then

10.          return  $X^{(0)};$ 

11.      endif

12. endfor

13. return  $X^{(0)};$ 

```

Algorithm 2. *Searching the optimal model X given N , K and B_g*

$X = LM(N, K, B_g)$

```

01.  randomly initialing  $\Gamma^{(0)} = (\gamma_{lk})_{L \times K}$  with  $\sum_k \gamma_{lk} = 1;$ 

02.   $s \leftarrow 1;$ 

```

03. *repeat until convergence:*

04. *compute $\Theta^{(s)}$, $\Delta^{(s)}$ and $\Omega^{(s)}$;*

05. *compute $\Gamma^{(s)}$;*

06. *$s \leftarrow s + 1$;*

07. *compute Z from $\Gamma^{(s)}$ according to Bayesian rule;*

Proposition 6. *Let B_{g_i} denotes the blocking model on the $i - th$ layer of the hierarchical organization of network N , we have:*

$$P(X|N, B_{g_1}, \dots, B_{g_h}) \propto P(N|X, B_{g_h})P(X)^{g_h}$$

Proof. $P(X|N, B_{g_1}, \dots, B_{g_h})$

$$= \frac{P(X, N, B_{g_1}, \dots, B_{g_h})}{P(N, B_{g_1}, \dots, B_{g_h})}$$

$$\propto P(X, N, B_{g_1}, \dots, B_{g_h})$$

$$= P(N|X, B_{g_1}, \dots, B_{g_h})P(X, B_{g_1}, \dots, B_{g_h})$$

$$= P(N|X, B_{g_1}, \dots, B_{g_h})P(X|B_{g_1}, \dots, B_{g_h})$$

$$P(B_{g_h}|B_{g_1}, \dots, B_{g_{h-1}}) \dots P(B_{g_2}|B_{g_1})P(B_{g_1})$$

$$\propto P(N|X, B_{g_1}, \dots, B_{g_h})P(X|B_{g_1}, \dots, B_{g_h})$$

Since two nodes from the same block of $B_{g_{i-1}}$ will also be in the same block of B_{g_i} , we have:

$$P(X|N, B_{g_1}, \dots, B_{g_h}) \propto P(N|X, B_{g_h})P(X|B_{g_h}) = P(N|X, B_{g_h})P(X)^{g_h}$$

□

Algorithm 3. *Computing the threshold of a blocking model based on Φ*

- 01. *sort all entries of Φ into a non-increasing sequence S ;*
- 02. *cluster all entries of Φ by the remarkable gaps of S ;*
- 03. *return the biggest entry of the cluster with the minimum*
mean as the threshold;

As examples, Fig. 5 illustrates, by means of the above algorithm, how to choose reasonable thresholds for reducing blocking models of the world trade net and the co-purchased political book network as discussed in the article.

B Additional Examples

Community detection from a benchmark network We have applied our approach to the football

association network, a benchmark widely used for testing the performance of community detection algorithms. Fig. 6 gives the experimental results.

Our approach automatically find out 10 clusters or communities from this network. Fig. 6(a) shows the clustered network, and Fig. 6(c1) shows the clustered matrix, in which dots denote the non-zero entries, and the rows and column corresponding to the same cluster will be put together and be separated by the solid lines. Fig. 6b shows the searching process, in which the cost in terms of $-L(N|X, B_1) + L_{OC}(X)$ firstly drops down quickly, and then goes up sharply after a local minimum corresponding to $K = 10$. This iterative searching process shapes a well-like landscape by penalizing both small likelihood and big coding complexity or smaller priori, and a good compromise between them is what we expect. Notice that, this estimated community number is a little bit smaller than the real one, in total 12 real associations, among which the teams from two small independent associations prefer to play matches with outside teams. (c)-(e) show the nested blocking models of this network. A hierarchical organization with three layers have been constructed.

Testing against synthetic networks We have tested our approach against several synthetic networks, and here we give two examples. Fig. 7a give one synthetic network, in which a 2-community pattern and two bipartite patterns coexist together. A two-layer nested organization are found out. In the first layer, six clusters with homogeneous row as well as column connection distributions are detected; in the second layer, such detected clusters are grouped in pairs according to the node couplings with coarser granularity. This time, a 2-community pattern, a reciprocal

bipartite pattern and an unilateral bipartite pattern are emerged. Fig. 7d give another synthetic network, in which 12 communities are organized in a 3-layer hierarchical structure according to the density of connections. Correspondingly, a three-layer nested blocking model is constructed as given in Fig. 7e.

Figure 1. An example of multiplex structures consisting of hubs, outliers, and communities co-existing in one social network. The network as shown in (a) depicts the co-appearances of 77 characters in the novel *Les Miserables* (by Victor Hugo). Nodes denote characters and links connect any pair of characters that appear in the same chapter of the novel. This data set is from *The Stanford GraphBase: A Platform for Combinatorial Computing*, edited by D.E.Knuth¹⁷. The physical connection profiles of nodes are represented in terms of the adjacency matrix as shown in (b), in which dots denote “1” entries. In total, six blocks are detected by our method in terms of the connection profiles of nodes, as separated by solid lines, so that the nodes within the same blocks will demonstrate homogeneous connectivities. To clearly visualize the block organization, the matrix has been transformed by putting together the nodes within the same blocks which are labeled by “block 1” to “block 6” from the top down. Correspondingly, in the network as shown in (a), nodes are also colored according to their block IDs (specifically, the coloring schema is: block 1-red, block 2-green, block 3-blue, block 4-cyan, block 5-gray and block 6-yellow), and the sizes of nodes are proportional to their respective degrees. (c) shows the blocking model of the network, in which each block is colored, numbered and placed according to the nodes it contains, and the sizes of blocks are proportional to the number of nodes they contain, respectively. The weights on the arrow lines globally measure the probabilities that one node from one block will connect to another from other blocks. (d) shows the reduced blocking model by cutting the arrow lines with trivial weights. In this case, one hub pattern consisting of block 1, one outlier pattern consisting of block 5 and four community patterns consisting of blocks 2,3,4 and 6 will readily be recognized by referring to the probabilistic linkage among these blocks.

Figure 2. The schematic illustrations of multiplex structures. (a)-(g) shows seven structural patterns frequently observed in real-world networks, which are represented by networks, matrices and blocking models, respectively. In the matrices, shades represent the densities of links. In the blocking models, circles denote blocks and solid arrow lines denote block feedforward-couplings. From (a)-(g), structural patterns are communities, authorities and outliers, hubs and outliers, a bow tie, a multipartite, a bipartite and a hierarchical organization, respectively. (g) shows a two-layer hierarchy; two overlapped communities (also can be seen as a hub with two communities) and one bipartite are in the first layer; two communities are in the second layer.

Figure 3. Detecting the nested core-periphery organization and the cash flow patterns from a world trade net. The network as shown in (a) encodes the trade relationship among 80 countries. Nodes denote countries and arcs denote countries imported commodities from others. The physical connection profiles of nodes are represented in terms of its adjacency matrix as shown in (b), in which dots denote “1” entries. In total, six blocks are detected as separated by solid lines so that the nodes within the same blocks will demonstrate homogeneous row- and column- connection distributions. As before, the matrix has been transformed by putting together the nodes within the same blocks which labeled by “block 1” to “block 6” from the top down. Correspondingly, in the network shown in (a), nodes are colored according to their block IDs (specifically, block 1-green, block 2-yellow, block 3-cyan, block 4-red, block 5-gray and block 6-blue), and the sizes of nodes are proportional to their respective out-degrees. (c) shows the world map in which 80 countries are colored by the same coloring schema defined above. (d) shows the detected two-layer hierarchical organization, in which each block is colored by the same coloring schema defined

above and the sizes of blocks are proportional to the number of nodes they contain, respectively. In the first layer, a reduced blocking model is given by cutting the trivial block couplings. The arrow lines with weights denote the cash flows from the countries within one block to others. The cash flows from two hubs (blocks 4 and 1) are highlighted by thicker arrow lines, of which the thickness is proportional to their strength measured by respective block couplings. These highlighted cash flows would outline the backbone of the cash circulation in the world trade system. A macroscopic hub-outlier pattern on the second layer is detected; together with the microscopic hub-outlier patterns on the first layer, the whole trade system would demonstrate a nested core-periphery organization. (e) shows the multiplex structures discovered from the reduced blocking model on the first layer by a procedure of matching isomorphism subgraphs as defined before. These structural patterns are stored in their respective reservoirs labeled as authority, community, hub or outlier.

Figure 4. Mining granular association rules from a co-occurrence net. The network in (a) encodes the co-purchased relationship among 105 books, in which the nodes with large, median and small sizes are labeled by “liberal”, “conservative” and “neutral(including one unlabeled)”, respectively. A two-layer hierarchical organization is detected. In the first layer, seven blocks are detected. As before, the matrix as shown in (b) has been transformed by putting together the nodes within the same blocks which labeled by “block 1” to “block 7” from the top down. Correspondingly, in the network shown in (a), nodes are colored according to their block IDs (specifically, block 1-blue, block 2-red, block 3-gray, block 4-brown, block 5-green, block 6-cyan and block 7-yellow). In the blocking model as shown in (b), each block is colored by the same

coloring schema defined above, the sizes of blocks are proportional to the number of nodes they contain, respectively; the arrow lines to be reserved in its reduced blocking model are highlighted by thicker arrow lines. The blocking model and its corresponding matrix of the second layer are shown in (c), in which a global two-community structure is detected. The granularity of the network corresponding to different layers is given by g .

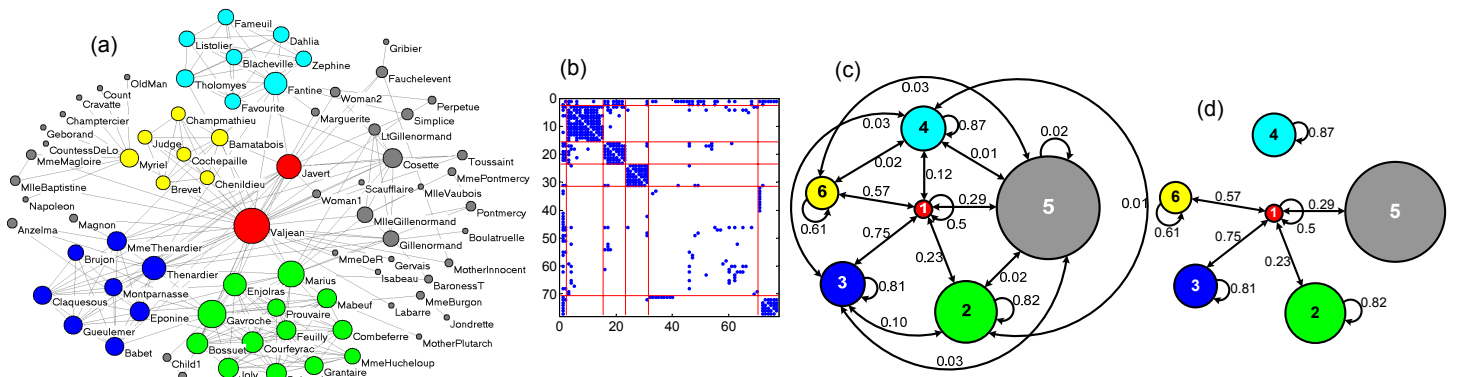


Figure 1: An example of the multiplex structures in a social network.

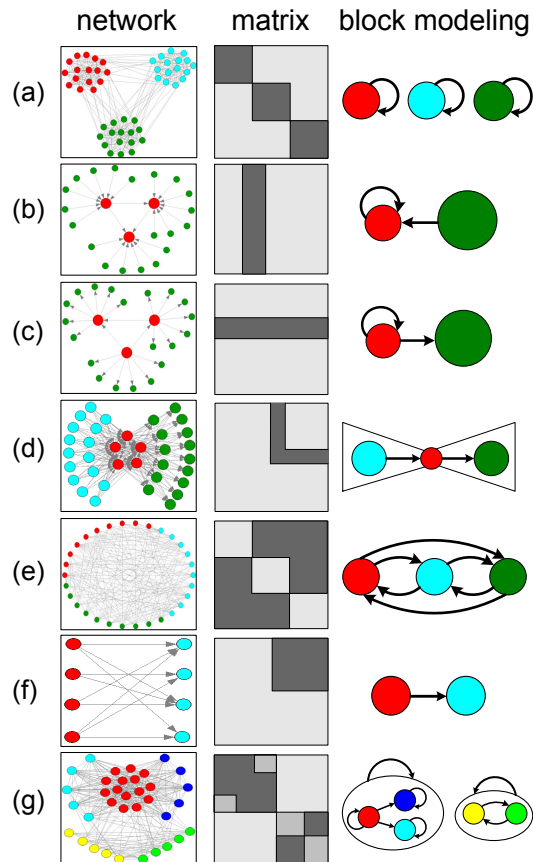


Figure 2: The schematic illustrations of multiplex structures.

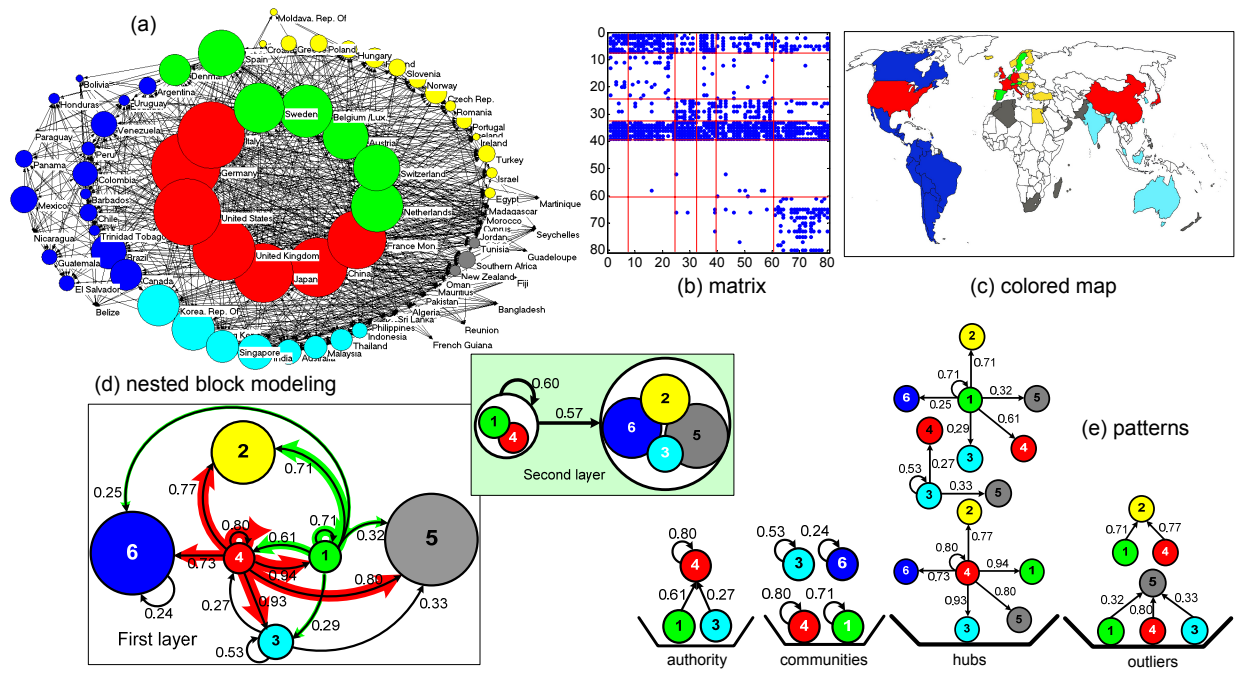


Figure 3: Detecting the nested core-periphery organization and the cash flow patterns from a world trade net.

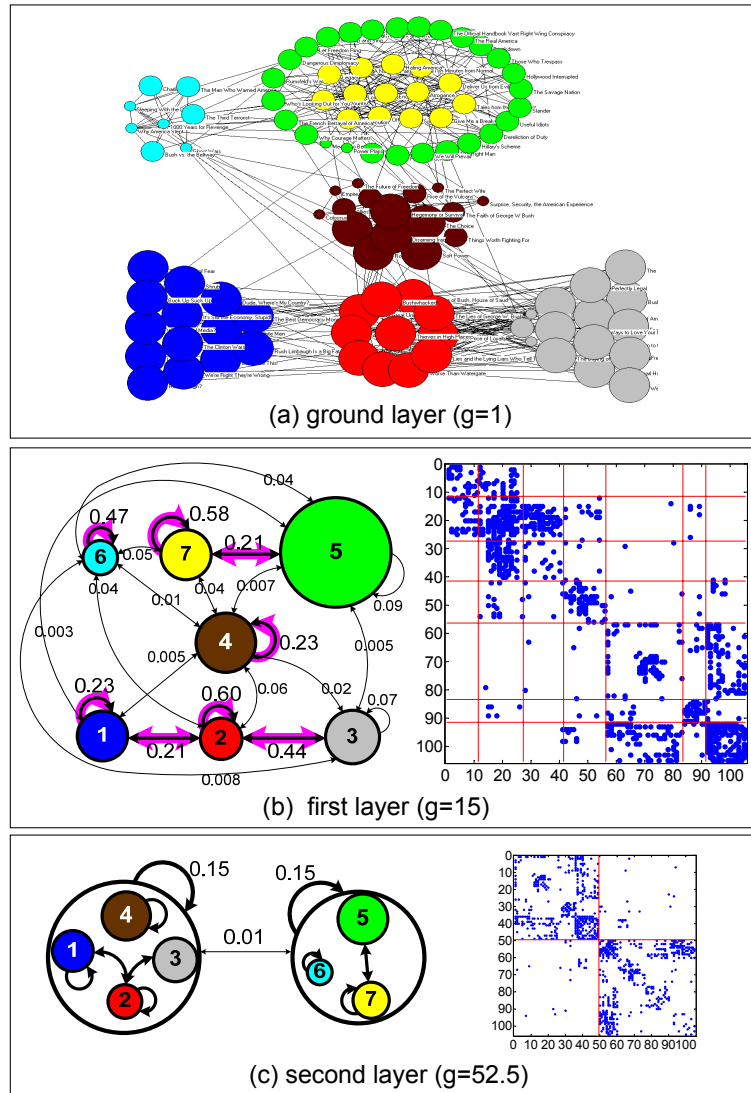


Figure 4: Mining granular association rules from a co-occurrence net.

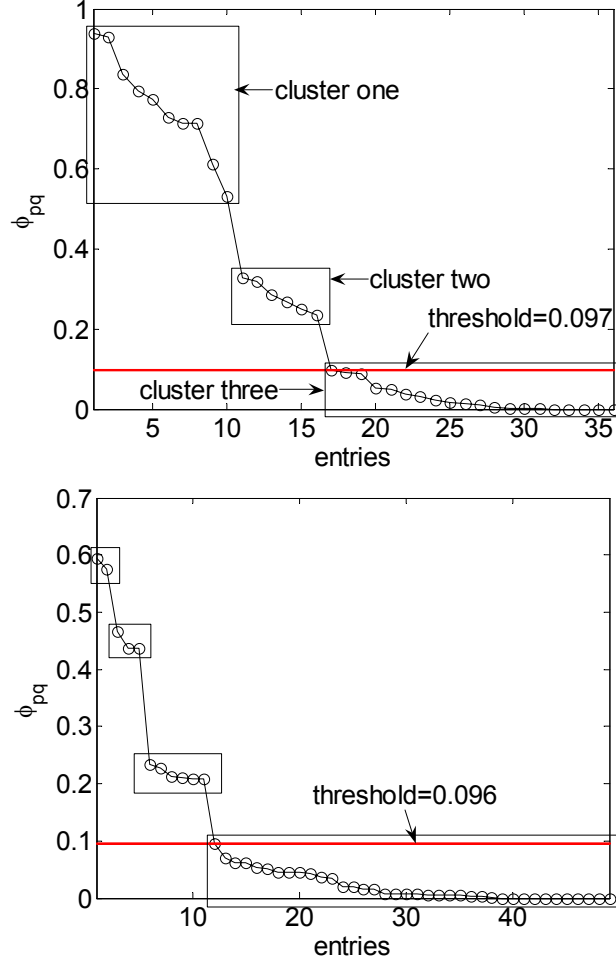


Figure 5: The illustrations of calculating thresholds for reducing blocking models. The top: calculating the threshold for the blocking model of the first layer of the world trade net. The bottom: calculating the threshold for the blocking model of the first layer of the co-purchased political book network. In both figures, the x denotes the sorted entries and the y denotes the values of block couplings in terms of Φ . These couplings are clustered into three or four groups, as separated by rectangles, by remarkable gaps. The calculated thresholds are the maximum entries of the clusters with minimum means pointed out by red solid lines, respectively.

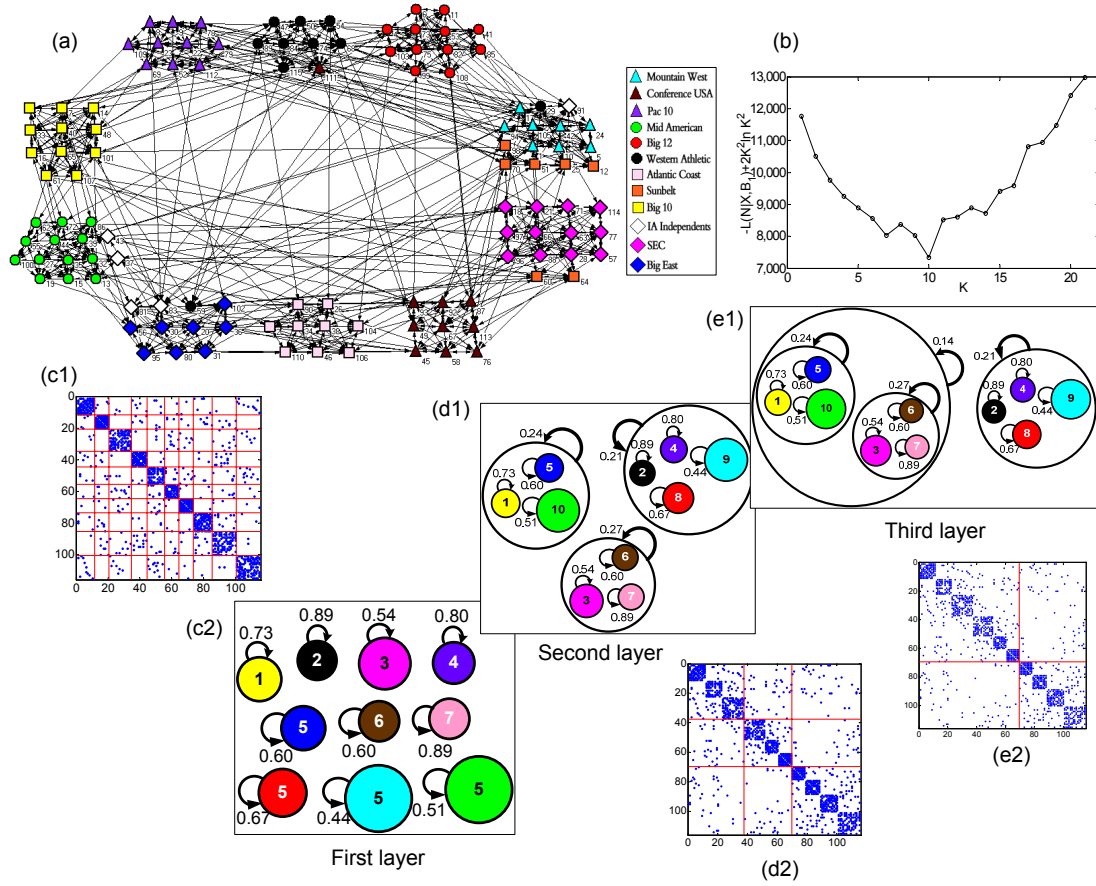


Figure 6: Detecting communities from the football association network. (a) The clustered football association network; (b) The iterative searching landscape. (c1-c2) The matrix and blocking model of the first layer. (d1-d2) The matrix and blocking model of the second layer. (e1-e2) The matrix and blocking model of the third layer. The coloring schemes used in (a) and (c2), (d1) and (e1) are same.

